On the nature of yrast states in neutron-rich polonium isotopes

R. Lică,[1,*] A.N. Andreyev,[2] H. Naïdja,[3] A. Blazhev,[4] P. Van Duppen,[5] B. Andel,[6] A. Algora,[7,8] S. Antalic,[6] J. Benito,[9] G. Benzoni,[10] T. Berry,[11] M. J. G. Borge,[12] C. Costache,[1] J. G. Cubiss,[2] H. De Witte,[5] L. M. Fraile,[9] H. O. U. Fynbo,[13] P. T. Greenlees,[14] L. J. Harkness-Brennan,[15] M. Huyse,[5] A. Illana,[16] J. Jolie,[4] D. S. Judson,[15] J. Konki,[14] I. Lazarus,[17] M. Madurga,[18] N. Marginean,[1] R. Marginean,[1] C. Mihai,[1] R. E. Mihai,[1] P. Mosat,[6] J. R. Murias,[9,19] E. Nacher,[7] A. Negret,[1] R. D. Page,[15] A. Perea,[12] V. Pucknell,[17] P. Rahkila,[14] K. Rezynkina,[5,20] V. Sánchez-Tembleque,[9] K. Schomacker,[4] M. Stryjczyk,[5,14] C. Sürder,[21] O. Tengblad,[12] V. Vedia,[9] and N. Warr[4]

(IDS Collaboration)

[1] *Horia Hulubei National Institute for R&D in Physics and Nuclear Engineering, RO-077125 Bucharest, Romania*
[2] *School of Physics, Engineering and Technology, University of York, York, YO10 5DD, United Kingdom*
[3] *Université Constantine 1, Laboratoire de Physique Mathématique et Physique Subatomique, Constantine 25000, Algeria*
[4] *Institut für Kernphysik, Universität zu Köln, D-50937 Köln, Germany*
[5] *KU Leuven, Instituut voor Kern- en Stralingsfysica, B-3001 Leuven, Belgium*
[6] *Department of Nuclear Physics and Biophysics, Comenius University in Bratislava, 84248 Bratislava, Slovakia*
[7] *Instituto de Física Corpuscular, CSIC - Universidad de Valencia, E-46980, Valencia, Spain*
[8] *Institute of Nuclear Research (ATOMKI), P.O.Box 51, H-4001 Debrecen, Hungary*
[9] *Grupo de Fìsica Nuclear, EMFTEL & IPARCOS, Universidad Complutense de Madrid, 28040 Madrid, SPAIN*
[10] *Istituto Nazionale di Fisica Nucleare, Sezione di Milano, I-20133 Milano, Italy*
[11] *Department of Physics, University of Surrey, Guildford GU2 7XH, United Kingdom*
[12] *Instituto de Estructura de la Materia, CSIC, Serrano 113 bis, E-28006 Madrid, Spain*
[13] *Department of Physics and Astronomy, Aarhus University, DK-8000 Aarhus C, Denmark*
[14] *University of Jyväskylä, Department of Physics, Accelerator laboratory, P.O. Box 35(YFL) FI-40014 University of Jyväskylä, Finland*
[15] *Department of Physics, Oliver Lodge Laboratory, University of Liverpool, Liverpool L69 7ZE, United Kingdom*
[16] *Instituto Nazionale di Fisica Nucleare, Laboratori Nazionali di Legnaro, I-35020 Legnaro, Italy*
[17] *STFC Daresbury, Daresbury, Warrington WA4 4AD, United Kingdom*
[18] *Dept. of Physics and Astronomy, University of Tennessee, Knoxville, Tennessee 37996, US*
[19] *Institut Laue-Langevin, CS 20156, 38042 Grenoble Cedex 9, France*
[20] *Université de Strasbourg, CNRS, IPHC UMR7178, F-67000, Strasbourg, France*
[21] *Institut für Kernphysik, Technische Universität Darmstadt, D-64289 Darmstadt, Germany*

(Dated: July 10, 2024)

Polonium isotopes having two protons above the shell closure at $Z = 82$ show a wide variety of low-lying high-spin isomeric states across the whole chain. The structure of neutron-deficient isotopes up to ^{210}Po ($N = 126$) is well established as they are easily produced through various methods. However, there is not much information available for the neutron-rich counterparts for which only selective techniques can be used for their production. We report on the first fast-timing measurements of yrast states up to the 8^+ level in ^{214,216,218}Po isotopes produced in the β^- decay of ^{214,216,218}Bi at ISOLDE, CERN. In particular, our new half-life value of 607(14) ps for the 8_1^+ state in ^{214}Po is nearly 20 times shorter than the one available in literature and comparable with the newly measured half-lives of 409(16) and 628(25) ps for the corresponding 8_1^+ states in ^{216,218}Po, respectively. The measured $B(E2; 8_1^+ \to 6_1^+)$ transition probability values follow an increasing trend relative to isotope mass, reaching a maximum for ^{216}Po. The increase contradicts the previous claims of isomerism for the 8^+ yrast states in neutron-rich ^{214}Po and beyond. Together with the other measured yrast transitions, the $B(E2)$ values provide a crucial test of the different theoretical approaches describing the underlying configurations of the yrast band. The new experimental results are compared to shell-model calculations using the KHPE and H208 effective interactions and their pairing modified versions, showing an increase in configuration mixing when moving towards the heavier isotopes.

Nuclear isomers are excited meta-stable states with half-lives of the order of nanoseconds and longer. The isomerism is usually caused by large differences between initial and final states in physical properties such as total angular momentum, its projection on the symmetry axis (K-isomers), shape, seniority or the low energy difference between the states [1, 2]. By determining the decay energy, branching ratio of de-exciting transitions and half-life of the state in question, one can deduce the reduced transition probability (a measure of the decay strength) and compare it to the single-particle estimate (which assumes that the decay involves a single nucleon). The ratio of the experimental and single-particle values defines a hindrance (or enhancement) factor which is related to the underlying decay mechanism. The occurrence of isomeric states in the vicinity of doubly-magic shell closures represents one of the important benchmarks for testing the predictive power of the nuclear shell model using different residual nucleon-nucleon interaction [3].

In the region around the doubly-magic $^{208}_{82}\mathrm{Pb}_{126}$, low-energy nuclear structure is often dominated by a relatively high-j single-particle orbital (with $j \geq 7/2$). Seniority (ν) represents the number of particles that are not paired (i.e., they are not coupled to angular momentum $J = 0$) and can be regarded as a good quantum number. Seniority isomers arise due to the selection rules associated with the conservation of ν and are encountered in semi-magic nuclei because electric quadrupole ($E2$) transitions between $\nu = 2$ states (*e.g.* $8^+_1 \to 6^+_1$) are small when the valence shell is close to half-filled [4].

Polonium isotopes, having two protons in the $h_{9/2}$ orbital above the $Z = 82$ shell closure, are especially suitable for testing the seniority scheme across the long chain of isotopes, also crossing the $N = 126$ shell closure. A large bulk of data exists in the literature on excited states and reduced transition probabilities $B(E2)$ in neutron-deficient $^{198-208}$Po isotopes. These nuclei can be studied through fusion-evaporation reactions with heavy ions [5, 6], Coulomb excitation experiments [7, 8] or β^+/EC decay [9]. These studies generally agree that the yrast structure (including the 8^+ seniority isomers) in the neutron-deficient polonium isotopes is dominated by the two-proton configuration $\pi(h_{9/2})^2$ coupled to the quadrupole vibrations of the underlying even-even ^{208}Pb core [10–12].

For isotopes heavier than ^{210}Po, the high-j neutron orbital $\nu(g_{9/2})$ starts to be filled. It is therefore expected to compete with the $\pi(h_{9/2})^2$ in determining the configuration of $0^+ - 8^+$ yrast states. The experimental studies of neutron-rich nuclei with $Z > 82$ and $N > 126$ are more challenging, as only very specific production techniques can be employed. One of the methods to populate excited states in such nuclei is through multi-nucleon transfer reactions such as $^{18}\mathrm{O} + {}^{208}\mathrm{Pb}$, used to study ^{210,212,214}Po [13–16].

A recent study of ^{214}Po [14] reported its yrast 8^+ state half-life of 13(1) ns and $B(E2; 8^+_1 \to 6^+_1) = 0.54(4)$ W.u., underlining its isomeric character. Based on the resemblance between the excitation energies of yrast states in ^{214,216,218}Po, the authors proposed that similar isomers might exist in ^{216,218}Po, their main excitation mechanism being one-neutron-pair breaking.

To reach isotopes beyond ^{214}Po, high-energy fragmentation or spallation in direct or inverse kinematics are the only methods of choice [17, 18]. In the past, by using proton-induced spallation in ^{232}Th and ^{238}U at ISOLDE, CERN, yrast states in ^{216,218}Po up to 8^+ have been populated through the β^- decay of ^{216,218}Bi [19, 20], however, half-life measurements of excited states were not performed.

In this Letter, we report on the first fast-timing measurements of the yrast $2^+, 4^+, 6^+$ and 8^+ states in ^{214,216,218}Po populated in the β^- decay of ^{214,216,218}Bi at ISOLDE, CERN. The present results strongly disagree with the previous literature value of the $T_{1/2}(8^+_1)$ in ^{214}Po [14]. The extracted $B(E2)$ values are compared to state-of-the-art shell-model calculations in order to understand the underlying structure of the yrast bands of ^{214,216,218}Po leading to a comprehensive characterization of the single-particle excitations in the "north-east" region of ^{208}Pb in the nuclear chart. We note that the detailed discussion of the decay schemes and newly-identified states in ^{214,216}Po from the same experiment has been recently reported for the β^- decay of ^{214}Bi [21] and ^{216}Bi [22].

The ^{214,216,218}Bi isotopes were produced at ISOLDE-CERN [23] by bombarding a $50\,\mathrm{g/cm^2}$ thick UC_x target with the 1.4 GeV proton beam delivered by the Proton Synchrotron Booster. The bismuth atoms released from the target were selectively ionized by the Resonance Ionization Laser Ion Source (RILIS), accelerated to 50 keV and mass-separated using the ISOLDE High Resolution Separator.

The bismuth ions were implanted on an aluminised Mylar® tape at the center of the ISOLDE Decay Station (IDS) detection setup equipped with a fast EJ232 plastic scintillator used as a β detector, four HPGe Clover detectors for the detection of γ rays in the daughter nuclei, and two small-volume ($30.5\,\mathrm{cm^3}$) conic $\mathrm{LaBr_3}$(Ce) detectors. This detection setup enabled the measurement of nuclear half-lives using the $\beta\gamma(t)$, $\gamma\gamma(t)$ and $\beta\gamma\gamma(t)$ fast-timing method [24, 25], a well established technique at IDS [26–29]. It covers half-lives between 10 ps and 100 ns by using fast-timing detectors such as $\mathrm{LaBr_3}$(Ce) and plastic scintillators in coincidence with HPGe detectors. More details about the calibration procedure of the detectors is provided in the Supplemental Material [30].

Energy spectra recorded by the HPGe and $\mathrm{LaBr_3}$(Ce) detectors in coincidence with β^- events are shown in Fig. 1. The production yields of ^{214,216,218}Bi ions were measured to be $> 2 \times 10^4$ (limited in order to reduce the count rate in the detectors), 1.5×10^3 and 2×10^2 ions/μC, respectively.

The half-lives of the 8^+_1 states in ^{214,216,218}Po were extracted through the $\beta\gamma\gamma(t)$ method by gating on β particles in the plastic scintillator as the START signal and the $8^+_1 \to 6^+_1$ γ-rays in the $\mathrm{LaBr_3}$(Ce) detectors as the STOP signal for the Time to Amplitude Converters. An extra gating condition was required on γ rays in the HPGe detectors originating from any of the three transitions below the 6^+_1 levels ($6^+_1 \to 4^+_1, 4^+_1 \to 2^+_1$ and $2^+_1 \to 0^+_1$)

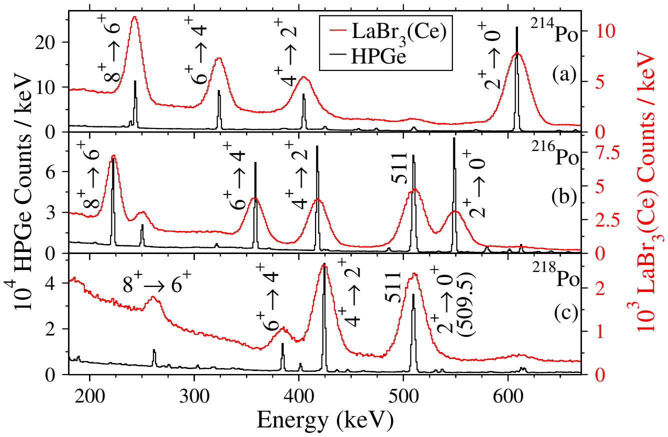

FIG. 1. β-gated γ-ray spectra recorded by the HPGe (black) and $LaBr_3(Ce)$ (red) detectors following the β^- decay of ^{214}Bi (a), ^{216}Bi (b) and ^{218}Bi (c). The yrast transitions in ^{214,216,218}Po are labeled.

in order to further reduce the background of resulting time-difference distributions, shown in Fig. 2 (a-c).

The possible delayed contributions from high-lying long-lived levels feeding the 8_1^+ states were investigated by HPGe gating on the γ-ray transitions from above. In the case of ^{214,216}Po, we report half-lives of 73(7) and 155(14) ps for the 8_2^+ 1824.5- [21] and 1802.6-keV [19] levels, respectively. For ^{218}Po, no long-lived states feeding the 8_1^+ level were identified, either because of the lack of statistics or their absence. The $LaBr_3(Ce)$ detectors cannot resolve the transitions feeding (240 keV) and de-exciting (244 keV) the yrast 8^+ state in ^{214}Po, see Fig. 1 (a), however, the two contributions were taken into account for the half-life analysis. The values of the half-lives reported in Table I are corrected for the contributions mentioned above and result from the convolution fit between a Gaussian (prompt response of the fast-timing detectors), an exponential decay and a flat background.

The time distributions for the decays of 2_1^+, 4_1^+, 6_1^+ states in ^{214,216,218}Po are shown in Fig. 2 (d-l). The deduced half-lives are reported in Table I and have been measured through the $\gamma\gamma(t)$ method by extracting the timing information from the $LaBr_3(Ce)$ detectors for γ rays directly populating and de-populating each level.

In the case of ^{214}Po, a significant discrepancy is observed between the newly measured half-life value of $T_{1/2}(8_1^+) = 607(14)$ ps, and the previous one of 13(1) ns [14]. The latter was measured using the slope fitting of time-difference distributions from HPGe detectors, known for having a much slower and less accurate time response compared to the $LaBr_3(Ce)$ detectors.

To link the newly measured data to the underlying nuclear structure, two effective interactions were used in the present work for the calculation of low-energy levels and $E2$ transition rates: (i) the recently-developed

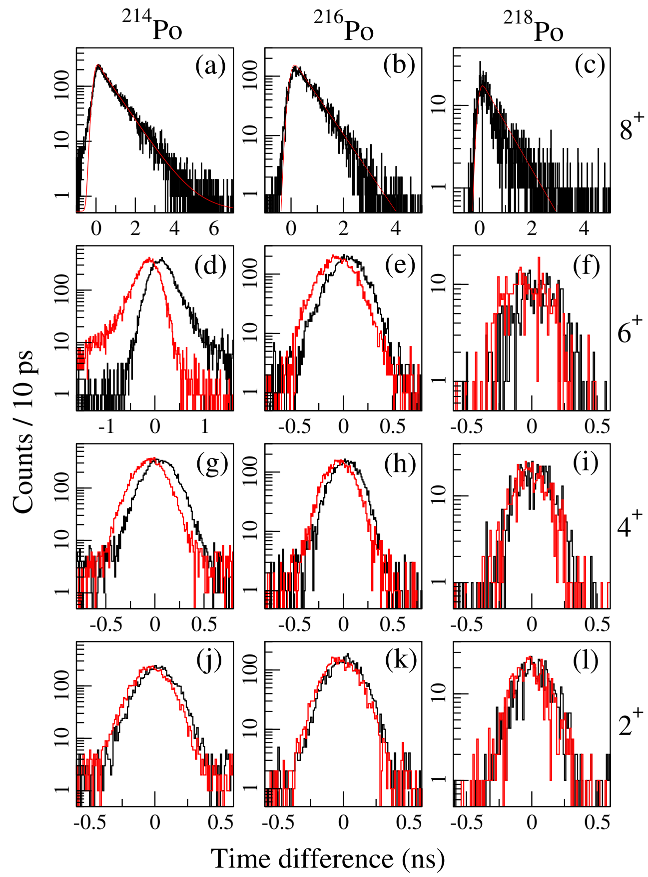

FIG. 2. (a-c) Background-subtracted time difference distributions between β particles recorded in the fast plastic scintillator and γ rays directly depopulating the yrast 8^+ states in ^{214,216,218}Po, extracted from β-γ_{La}-γ_{Ge} events. (d-l) Delayed (black) and anti-delayed (red) background-subtracted time distributions between γ rays directly feeding and de-exciting the yrast 2^+, 4^+ and 6^+ states in ^{214,216,218}Po, extracted from γ_{La}-γ_{La} events. The half-lives, reported in Table I, were measured using the decay slope method (a-c) and the centroid-shift method (d-l) [24, 25]. The longer lived component (tail) in the ^{214}Po 6^+ spectrum (d) originates from the 8^+ half-life due to an overlap in the LaBr3(Ce) energy spectra between the feeding (240 keV) and de-exciting (245 keV) transitions. However, it was excluded when evaluating the centroid shift of the distribution.

H208 effective interaction [3, 31] already used in the interpretation of ^{212,214,216}Po new experimental data [21, 22, 32, 33]; (ii) the well-established Kuo-Herling interaction as modified by Warburton and Brown [34], denoted as KHPE. More details regarding the calculations are provided in the Supplemental Material [30].

Additional modifications of the two interactions, denoted by H208-m and KHPE-m, were implemented within this work in order to reconcile calculated and experimental $B(E2)$ values. Specifically, the diagonal and off-diagonal $1h_{9/2}$ proton-pairing matrix elements were reduced by 100 keV in H208-m. The KHPE-m reduction was 100 keV for ^{218}Po and 200 keV for $^{210-216}$Po (for a similar 200-keV reduction in ^{218}Po, the 8_1^+ state excitation energy becomes lower than the 6_1^+ one). The $1h_{9/2}0i_{13/2}$ matrix elements were not modified, as they had an insignificant effect on the studied $E2$ transitions.

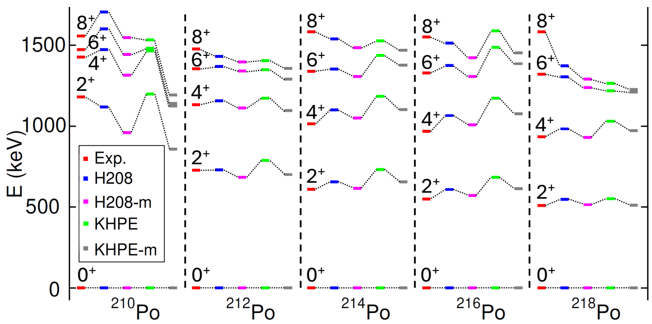

FIG. 3. The calculated $0^+ - 8^+$ yrast energy levels of even-even $^{210-218}$Po isotopes using H208, H208-m, KHPE and KHPE-m interactions, compared to the available experimental data [14, 35–39].

By comparing the excitation energies of calculated and experimental $0^+ - 8^+$ yrast levels in $^{210-218}$Po isotopes, shown in Fig. 3, we notice that the H208 interaction is in better agreement with the adopted experimental data [36–39] than KHPE, except for ^{210}Po [35]. A common shortcoming is a compression by about 200 keV observed for the 8_1^+ state of ^{218}Po, which we attribute to the adopted truncation for that nucleus.

In order to investigate in detail the wave function structure of the yrast states, Table II in the Supplemental Material [30] reports their main components (with ≥ 10% contribution), where we note the following points: (i) all the yrast $2^+ - 8^+$ states in ^{210}Po ($N = 126$) have nearly pure proton $1h_{9/2}$ contribution; (ii) for $N > 126$ the contribution from the pure $1h_{9/2}$ diminishes, and the composition is more fragmented. The neutron $1g_{9/2}$ state starts to play a strong role in all the yrast states, *e.g.* nearly 54% in $0^+ - 6^+$ in ^{212}Po, and with a further admixture of $1f_{7/2}$ proton for the 8_1^+ state. An even more fragmented wave function can be seen for $^{214-218}$Po, with the added contribution from the $0i_{11/2}$ neutron orbital.

The calculated $B(E2; J^\pi \to (J-2)^\pi)$ reduced transition probabilities interconnecting the yrast $0^+ - 8^+$ states are compared to our new results and to available data from literature [14, 15, 35, 36, 40] in Fig. 4, Table I here and Table I in the Supplemental Material [30]. The results of the H208 and KHPE calculations are close to each other, with the exception of ^{218}Po, where different truncations are implemented. Overall, they are within error bars with the new measurements, with few exceptions mentioned below.

We first note the over-estimation of the $B(E2, 2_1^+ \to 0_1^+)$ values in ^{210,212,214}Po isotopes by a factor of two. However, the calculated $B(E2; 4_1^+ \to 2_1^+)$ and $B(E2; 6_1^+ \to 4_1^+)$ values are very well reproduced by the

			$B(E2; J^\pi \to (J-2)^\pi)$ (W.u.)				
Nucl.	J^π	$T_{1/2}$ (ps) Exp.	Exp.	H208	H208 -m	KHPE	KHPE -m
^{214}Po	2_1^+	13(5)	7(3)	13.6	14.3	12.3	13.2
	4_1^+	35(5)	18(3)	16.9	18.5	13.3	16.5
	6_1^+	118(5)	16(1)	11.4	14.7	5.9	12.6
	8_1^+	607(14)	11.3(3)	1.2	9.2	0.1	6.6
		13(1) ns	**0.54(4)**[14]				
^{216}Po	2_1^+	11(5)	13(6)	18.1	18.9	17.7	18.7
	4_1^+	21(5)	26(6)	25.2	27.1	22.1	25.2
	6_1^+	31(5)	37(6)	18.8	25.0	9.8	23.2
	8_1^+	409(16)	24(1)	16.2	17.8	3.2	15.5
^{218}Po	2_1^+	<15	>13	19.2	20.1	14.8	15.3
	4_1^+	<15	>33	29.9	31.5	21.5	22.9
	6_1^+	20(8)	40(16)	28.3	35.0	2.8	3.2
	8_1^+	628(25)	7.8(3)	8.5	16.2	1.0	0.003

TABLE I. Experimental $T_{1/2}$ and $B(E2)$ values in $^{214-218}$Po measured in the present work and Ref. [14] (bold), compared to calculated $B(E2)$s using various effective interactions: H208, KHPE, and their pairing-modified versions.

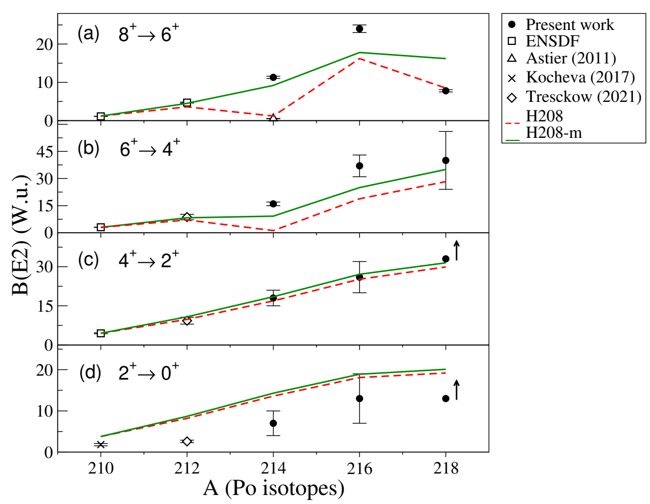

FIG. 4. $B(E2; J^\pi \to (J-2)^\pi)$ values for transitions between ^{214,216,218}Po yrast states measured in the present work (full circles with uncertainties) and from adopted experimental values [35, 36] or the most recent experimental results [14, 15, 40]. The comparison with shell-model calculations using the H208 interaction initial and pairing-modified versions (colored lines) is presented. Lower limits for the experimental $B(E2)$ values are indicated with an arrow pointing up. All the values are reported in Table I.

shell-model calculations, shown in Table I, which suggests that the correct structure of the 2_1^+ state wave function was taken into account. This $B(E2, 2_1^+ \to 0_1^+)$ discrepancy was already explained in Refs. [34, 41] by the absence of the contribution from particle-hole core excitations in the 0_1^+ wave function and later, the α-cluster model was proposed [40].

The most striking discrepancy is observed for the $B(E2; 8_1^+ \to 6_1^+)$ values in ^{214}Po, where our newly measured value is at least 10 times larger than the original shell-model calculated one, questioning the isomeric nature of the 8^+_1 state in ^{214}Po. To understand the origin of this inconsistency between theory and our new measurements, the modified effective interactions were employed. As a consequence, there was a remarkable increase of the calculated $B(E2; 8^+_1 \to 6^+_1)$ value in ^{214}Po, from 1.2 to 9.2 W.u. in H208-m and from 0.1 to 6.6 W.u. in KHPE-m, close to the measured value of 11.3(3) W.u., as shown in Fig. 4 and Table I.

To provide a complementary insight into the effect of the aforementioned pairing modifications on the wave functions structure of the lowest states in ^{214}Po, the same calculations are performed in the seniority (ν) scheme using the j-coupled NATHAN code [42]. The results obtained using H208 and H208-m are displayed in Fig. 5, where $T(x, y)$ represents the number of neutron (x) or proton (y) pairs being broken (*e.g.* the 0^+_1 state wave-function is dominated by a 66% contribution from $T(0, 0)$ which corresponds to $\nu = 0$, and the 2^+_1 by 45% of $T(1, 0)$ corresponding to $\nu = 2$). No important change between the two versions can be observed in the seniority structure of the $0^+_1, 2^+_1, 4^+_1$ and 6^+_1 states. The effect of reducing the $1h_{9/2}$ proton pairing matrix elements is apparent on the structure of the two lowest 8^+ states. In H208, the main wave function component of the 8^+_1 state was characterized by seniority $\nu = 2$ (one neutron pair broken). The 8^+_2 state was initially predicted very close in energy to the 8^+_1 state, connected by a strong $E2$ transition to the 6^+_1 state and characterized by a mixing of ν=2, 4 and 6. Reducing the pairing in H208-m leads to an inversion of the $8^+_{1,2}$ states, the $\pi(1h_{9/2}1f_{7/2})$ state comes below the $\nu g^4_{9/2}$ 8^+ one, resulting in a good agreement between experiment and calculations.

The increasing trend of the experimental $B(E2; J^\pi \to (J-2)^\pi)$ values for transitions from the $J = 2, 4, 6, 8$ states, shown in Fig. 4, was predicted theoretically in neutron-rich Po isotopes up to $A = 216$, with the exception of a dip in ^{214}Po, for the $8^+_1 \to 6^+_1$ transition (see Figs. 6-9 from Ref. [3]). The trend was explained through the increase of the collectivity and quadrupole correlations with respect to the neutron number, leading to strong electromagnetic strengths.

The sudden decrease of the experimental $B(E2; 8^+_1 \to 6^+_1)$ for ^{218}Po is also reproduced theoretically, despite the adopted truncation in this nucleus. This can be attributed to the contribution from $i_{13/2}$ and $j_{15/2}$ proton and neutron orbitals in the structure of the 8^+_1 and 6^+_1 states. A strong transition probability of 27 W.u. is calculated when excluding the aforementioned orbitals. Their inclusion determines a reduction of quadrupole correlations due to pairing, leading to the $B(E2; 8^+_1 \to 6^+_1)$ decrease observed in ^{218}Po.

In conclusion, the $B(E2)$ transition probabilities of yrast states up to the 8^+ level in ^{214,216,218}Po isotopes populated in the β^- decay of ^{214,216,218}Bi are established for the first time through fast-timing measurements at the ISOLDE Decay Station. The comparison with shell-model calculations using the standard versions of the H208 and KHPE effective interactions shows reasonable agreement for the lower-lying transitions. A significant disagreement was observed in the case of the $8^+_1 \to 6^+_1$ transitions, especially for ^{214}Po where a much higher transition probability was measured ($B(E2) = 11.3(3)$ W.u. instead of 0.54(4) W.u. [14]), disproving its previously-claimed isomeric character. Similarly, based on the large $B(E2)$ values, the 8^+_1 states in $^{216-218}$Po should not be considered isomeric. An improved agreement between theory and the present measurement was achieved after reducing the pairing strength of the interactions, effectively inverting the lowest predicted 8^+ states and confirming the two-proton configuration $\pi(1h_{9/2}1f_{7/2})$ of the yrast 8^+ state dominated by quadrupole correlations. The new findings can serve as a guideline for future analysis, providing a clear indication of the nature of 8^+_1 states in neutron-rich polonium isotopes. Additionally, they serve as an extremely valuable input for the different theoretical approaches and constitute a stringent test for the effective interactions.

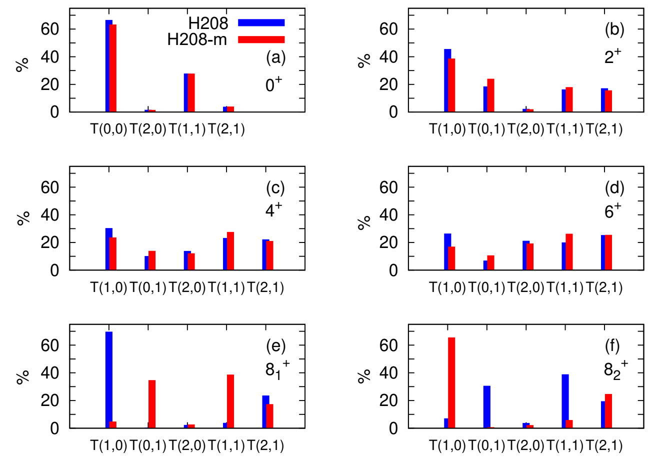

FIG. 5. The wave-function components of ^{214}Po states calculated in seniority scheme where $T(x, y)$ represents the number of neutron (x) or proton (y) pairs being broken. The initial and pairing-modified versions of the H208 effective interaction are employed within the NATHAN code.

We would like to thank B.A. Brown, A. Gargano and the late H. Grawe for the inspiring discussions and the ISOLDE staff for the support provided during the experiment. We acknowledge support for this work by the Romanian IFA grant CERN/ISOLDE and Nucleu project No. PN 23 21 01 02, the Slovak Research and Development Agency (Contract No. APVV-22-0282) and the Slovak grant agency VEGA (Contract No. 1/0651/21), the

Research Foundation Flanders (FWO, Belgium), BOF KU Leuven (C14/22/104), fWO and F.R.S.-FNRS under the Excellence of Science (EOS 40007501) programme, the Spanish MCIN/AEI/10.13039/ 501100011033 under grants RTI2018-098868-B-I00 and PID2021-126998OB-I00, the Academy of Finland project No. 354968, the German BMBF under contract 05P21PKCI1 and Verbundprojekt 05P2021, and the United Kingdom Science and Technology Facilities Council (STFC) through the grants ST/P004598/1 and ST/V001027/1.

* razvan.lica@nipne.ro

[1] S. Garg *et al.*, Atomic Data and Nuclear Data Tables **150**, 101546 (2023).
[2] P. Walker and G. Dracoulis, Nature **52**, 35 (1999).
[3] H. Naïdja, Phys. Rev. C **103**, 054303 (2021).
[4] P. V. Isacker, J. Phys.: Conf. Ser. **322**, 012003 (2011).
[5] A. Maj *et al.*, Nuclear Physics A **509**, 413 (1990).
[6] K. Stoychev *et al.*, Phys. Rev. C **108**, 014316 (2023).
[7] T. Grahn *et al.*, Eur. Phys. J. A **52**, 340 (2016).
[8] K. Wrzosek-Lipska and L. P. Gaffney, J. Phys. G: Nucl. Phys. **43**, 024012 (2016).
[9] N. Bijnens *et al.*, Phys. Rev. Lett. **75**, 4571 (1995).
[10] O. Häusser *et al.*, Nuclear Physics A **273**, 253 (1976).
[11] G. Neyens *et al.*, Nuclear Physics A **625**, 668 (1997).
[12] G. D. Dracoulis, P. M. Walker, and F. G. Kondev, Reports on Progress in Physics **79**, 076301 (2016).
[13] A. Astier *et al.*, Eur. Phys. J. A **46**, 165 (2010).
[14] A. Astier and M.-G. Porquet, Phys. Rev. C **83**, 014311 (2011).
[15] D. Kocheva *et al.*, Eur. Phys. J. A **53**, 175 (2017).
[16] D. Kocheva *et al.*, Phys. Rev. C **96**, 044305 (2017).
[17] G. Benzoni *et al.*, Phys. Lett. B **715**, 293 (2012).
[18] A. I. Morales *et al.*, Phys. Rev. C **89**, 014324 (2014).
[19] J. Kurpeta *et al.*, Eur. Phys. J. A **7**, 49 (2000).
[20] H. De Witte *et al.*, Phys. Rev. C **69**, 044305 (2004).
[21] B. Andel *et al.* (IDS Collaboration), Phys. Rev. C **104**, 054301 (2021).
[22] B. Andel *et al.* (IDS Collaboration), Phys. Rev. C **109**, 064321 (2024).
[23] M. J. G. Borge and B. Jonson, J. Phys. G: Nucl. Phys. **44**, 044011 (2017).
[24] M. Moszynski and H. Mach, NIM A **277**, (1989).
[25] H. Mach, R. L. Gill, and M. Moszynski, NIM A **280**, 49 (1989).
[26] L. M. Fraile, J. Phys. G: Nucl. Phys. **44**, 094004 (2017).
[27] R. Lică *et al.* (IDS Collaboration), Phys. Rev. C **93**, 044303 (2016).
[28] R. Lică *et al.*, J. Phys. G: Nucl. Phys. **44**, 054002 (2017).
[29] R. Lică *et al.* (IDS Collaboration), Phys. Rev. C **97**, 024305 (2018).
[30] See Supplemental Material at [URL will be inserted by publisher] for additional details about the detector calibration procedure and shell-model calculations.
[31] H. Naïdja, Physica Scripta **94**, 014005 (2018).
[32] A. Fernández *et al.*, Phys. Rev. C **104**, 054316 (2021).
[33] V. Karayonchev *et al.*, Phys. Rev. C **106**, 064305 (2022).
[34] E. K. Warburton and B. A. Brown, Phys. Rev. C **43**, 602 (1991).
[35] M. Shamsuzzoha Basunia, NDS **121**, 561 (2014).
[36] K. Auranen and E. McCutchan, NDS **168**, 117 (2020).
[37] S. Zhu and E. McCutchan, NDS **175**, 1 (2021).
[38] S.-C. Wu, NDS **108**, 1057 (2007).
[39] B. Singh *et al.*, NDS **160**, 405 (2019).
[40] M. von Tresckow *et al.*, Phys. Lett. B **821**, 136624 (2021).
[41] V. Karayonchev *et al.*, Phys. Rev. C **99**, 024326 (2019).
[42] E. Caurier and F. Nowacki, unpublished.